

Title	High-resolution Observation of Polymer Single Crystals with a Superconducting Cryo-TEM (Commemoration Issue Dedicated to Professor Ken-ichi Katayama On the Occasion of His Retirement)
Author(s)	Tsuji, Masaki; Tosaka, Masatoshi; Kawaguchi, Akiyoshi; Katayama, Ken-ichi; Iwatsuki, Masashi
Citation	Bulletin of the Institute for Chemical Research, Kyoto University (1991), 69(2): 117-126
Issue Date	1991-09-14
URL	http://hdl.handle.net/2433/77380
Right	
Type	Departmental Bulletin Paper
Textversion	publisher

High-resolution Observation of Polymer Single Crystals with a Superconducting Cryo-TEM

Masaki TSUJI[†], Masatoshi TOSAKA^{††}, Akiyoshi KAWAGUCHI,
Ken-ichi KATAYAMA and Masashi IWATSUKI*

Received June 26, 1991

The appreciable effectiveness of cryo-protection in high-resolution imaging of radiation-sensitive polymer crystals with a transmission electron microscope [TEM] was demonstrated by comparing the total end-point dose [TEPD] at 4.2k with that at room temperature, where TEPD means an electron dose needed for complete destruction of crystallinity of a specimen by electron irradiation. As the specimens, solution-grown single crystals of polyethylene, poly(4-methyl-1-pentene) form-III and poly(bisphenoxyphosphazene) α -form were used. By grace of the increase in TEPD by cryo-protection, high-resolution TEM images of three kinds of specimens mentioned above were successfully obtained at 4.2k using a cryo-TEM with a superconducting objective lens.

KEY WORDS: Radiation damage, Cryo-protection, Lattice image, Molecular image, Image processing, Polyethylene, Poly(4-methyl-1-pentene), Poly(bisphenoxyphosphazene),

INTRODUCTION

Present-day transmission electron microscopes [TEM] are widely used in order to clarify the atomic or molecular arrangement in crystalline materials, provided that the materials are resistant enough against electron irradiation. Though most of the polymer crystals are vulnerable to electron bombardment, several high-resolution TEM works have been reported so far for some polymers at room temperature mostly with a conventional 100~200kV instrument. In particular, the high-resolution image of poly(*p*-xylylene) [PPX] single crystal of β -form revealed the molecular arrangement in the unit cell, being utilized for the structure analysis of the β -form crystal¹⁾. The lattice images of poly(*p*-phenylene terephthalamide)²⁾, PPX³⁾ and poly(aryl-ether-ether-ketone) [PEEK]⁴⁾ directly demonstrated the crystallite orientation/size in their oriented films, and their curved lattice fringes suggested the lattice distortion accompanied with bending of chain stems. In the case of some radiation-sensitive polymers, lattice images of isotactic polystyrene⁵⁾, cellulose⁶⁾, α -chitin⁷⁾, poly(tetrafluoroethylene)⁸⁾ and polyethylene [PE]⁹⁾, and molecular images of β -chitin¹⁰⁾, poly(tetramethyl-*p*-silphenylene siloxane)¹¹⁾ and poly(β -hydroxybutyrate)¹²⁾

辻 正樹[†], 登阪 雅聡^{††}, 河口 昭義, 片山 健一; Laboratory of Polymer Crystals, Institute for Chemical Research, Kyoto University, Uji, Kyoto-fu 611, Japan.

* 岩槻 正志; SA Group, JEOL Ltd., Akishima, Tokyo-to 196, Japan.

† To whom correspondence should be addressed.

†† Present address: Plastic Optical Devices Technology Group, Plastic Products Technical Center, Asahi Chemical Industry Co. Ltd., Kawasaki, Kanagawa-ken 210, Japan.

were successfully obtained using a low-dose technique with a minimum dose system [MDS]¹³⁾ installed in JEOL TEM's or with a low dose unit [LDU]¹⁴⁾ in Philips ones. The low-dose technique is, however, a method to avoid electron irradiation of specimens except at image recording. Even if with the MDS or LDU, it is still rather difficult to take high-resolution images of most of the polymer specimens which will lose their crystallinity at a dose less than some hundreds of electrons/nm².

There are two ways to extend the life span of crystalline state of the specimens under electron irradiation; (1) to raise accelerating voltage of TEM, and (2) to cool the specimens down to a low temperature in TEM ("cryo-protection"). In this communication, the effectiveness of cryo-protection in high-resolution imaging of polymer crystals is discussed, and some results using a cryo-TEM with a superconducting objective lens are presented.

EXPERIMENTAL

Samples

The specimens used in this study are single crystals of PE, poly(4-methyl-1-pentene) [P4M1P] and poly(bisphenoxyphosphazene) [PBPP] grown from respective solutions.

The lozenge-shaped single crystals of PE were grown isothermally at 86°C from a 0.01% solution of "NBS SRM-# 1483(M_w~32,100)" in *p*-xylene.

The square single crystals of P4M1P form-III¹⁵⁾ were kindly supplied by Dr. R. St. John Manley, Pulp and Paper Research Institute of Canada and Department of Chemistry, McGill University, as a suspension in a sealed glass tube. The crystals were grown isothermally at 63°C from a 0.03% solution in xylene.

The lath-shaped single crystals of PBPP α -form¹⁶⁾ were kindly supplied by Dr. M. Kojima, Chisso Corporation, as a suspension. The crystals were grown isothermally at 60°C for 20 hours from a 0.015% solution in xylene.

Electron microscopy

Morphological observation and electron diffraction [ED] experiments were carried out at room temperature using a JEOL JEM-200CS operated at 200kV. Cryogenic electron microscopy was performed at 4.2K using a JEOL JEM-2000SCM¹⁷⁾ with a superconducting objective lens, operated at 160kV for high-resolution imaging and 200kV for measuring the total end-point dose [TEPD] of the specimens. Here, the TEPD is defined as a dose needed for complete disappearance of all crystalline reflections in the ED pattern. TEPD at room temperature, however, was measured for the specimens using a JEOL JEM-2000FX operated at 200kV, which is a conventional TEM with the same device for measuring electron beam current as a JEM-2000SCM.

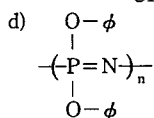
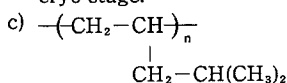
The specimens were deposited onto a carbon support-film mounted on a Cu grid, and then shadowed with Pt-Pd or Au for morphological observation. For ED experiments, Al, Ag or Au was evaporated onto some of the specimens as an internal reference material for calibrating the camera length. In the case of high-resolution observations, a very thin carbon support (<10nm in thickness) was used, which was

Table 1 Temperature dependence of TEPD at 200kV for the polymer single crystals used in this study

Polymer	$N_{RT}^{a)}$ [electrons/nm ²]	$N_{4.2}^{b)}$ [electrons/nm ²]	$N_{4.2}/N_{RT}$
PE	3.9×10^2	6.0×10^3	15
P4M1P ^{c)}	1.5×10^2	3.6×10^3	24
PBPP ^{d)}	1.5×10^2	2.1×10^4	140

a) N_{RT} is TEPD at room temperature, which was measured with a JEOL JEM-2000FX.

b) $N_{4.2}$ is TEPD at 4.2K, which was measured using a JEOL JEM-2000SCM equipped with a superconducting objective lens and a cryo-stage.



mounted on an Ag- or Au-coated Triafol "microgrid". In taking high-resolution images, MDS was used. All the ED patterns and images were recorded onto Mitsubishi electron microscope films [MEM].

RESULTS AND DISCUSSION

Table 1 shows the temperature dependence of TEPD for the specimens used in this study. In this table, $N_{4.2}$ and N_{RT} denote TEPD at 4.2k and that at room temperature, respectively. The ratio of $N_{4.2}/N_{RT}$ of more than 10 was confirmed for all the specimens used here¹⁹⁾. In 1982, Knapek reported the ratio of 10~300 for various materials using a cryo-TEM with a superconducting objective lens¹⁹⁾. Thereafter, Yamagishi *et al.* obtained the ratio of ca. 20 for t-RNA crystals, which was calculated from the critical doses measured using a specially designed TEM both at 7.9K and at room temperature for the reflection of 0.9nm spacing²⁰⁾. The N_{RT} 's of three kinds of specimens used here are 150~400 electrons/nm². These low values imply the difficulty in recording their high-resolution images on a photographic film. However, lattice images of single crystals of PE²¹⁾ and P4M1P²²⁾ and of highly oriented thin films of PE⁹⁾ were really obtained so far at room temperature with a conventional TEM operated at 120kV, although their image quality is not always high due to an extremely low dose for image recording. Now, the $N_{4.2}$ of PE, for example, increases up to the value equivalent to the N_{RT} of PEEK: an oriented thin film of PEEK gives a high-resolution image at room temperature, the optical diffraction [OD] pattern of which shows the 220 reflection corresponding to the lattice spacing of 0.236nm⁴⁾. Consequently, improvement of resolution limit is greatly expected for polymer crystals owing to the definite increase in TEPD by cryo-protection.

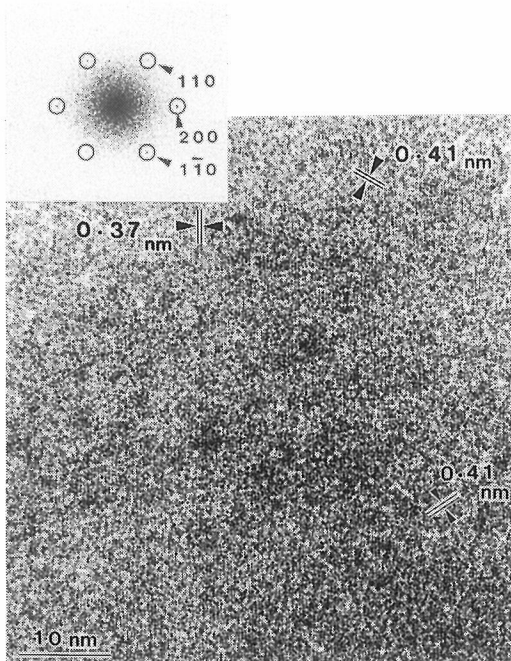


Fig. 1
High-resolution image of PE single crystal taken at 4.2K and $M=90,000$. The inset is the OD pattern of the image.

PE single crystal

Figure 1 shows a lattice image of the PE single crystal, which image was taken at 4.2K and an electron optical magnification of $M=90,000$. The OD pattern (the inset of Fig. 1) from the original negative shows 110, $1\bar{1}0$ and 200 reflections. In Fig. 1, (110) and ($1\bar{1}0$) lattice fringes of 0.41nm spacing and (200) fringes of 0.37nm spacing are actually identified. In particular, the (200) fringes are clear and seemingly straight over a fairly wide area. Some of the micrographs showed the 020 reflection of 0.25nm spacing with 110 or 200 in their OD patterns. Figure 2 demonstrates such an example: the OD pattern of the image (the inset of Fig. 2) shows 020, 110 and $1\bar{1}0$ reflections but no 200, probably

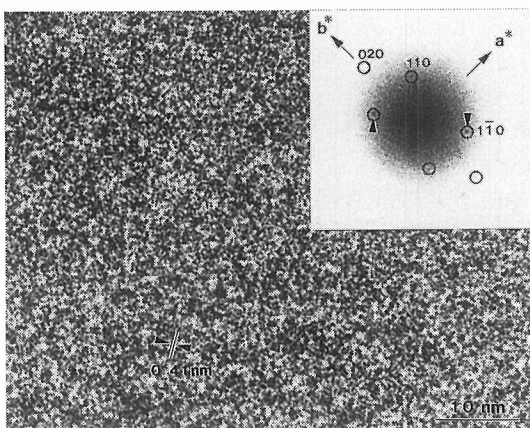


Fig. 2
High-resolution image of PE single crystal taken at 4.2K and $M=60,000$. The inset is the OD pattern of the image. The lattice fringes of 0.41nm spacing are recognized in the image.

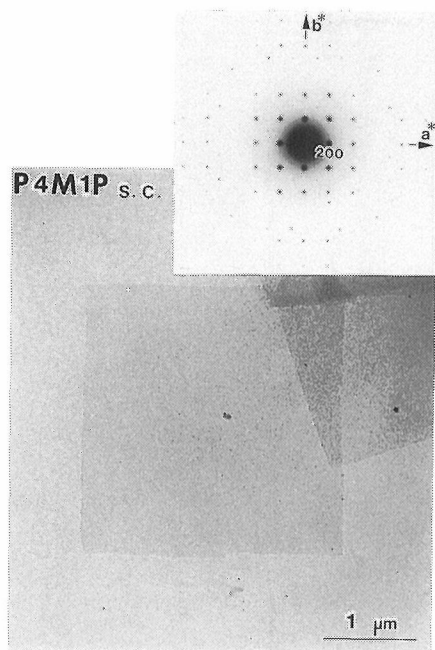


Fig. 3 P4M1P form-III single crystal shadowed with Pt-Pd. The inset is the corresponding ED pattern from the mono-layered crystal, showing that the chain axis(c -axis) is set normal to the basal surface of the single crystal platelet.

because the crystallites were tilted slightly around the b -axis so that no condition for imaging was fulfilled.

P4M1P single crystal

Figure 3 shows a square single crystal of P4M1P and the corresponding ED pattern. As concluded from ED patterns calibrated with diffraction rings of Ag, the crystals were assigned to form-III: tetragonal, $a=1.93\text{nm}$, $c(\text{chain axis})=0.698\text{nm}^{15}$.

Figure 4 shows a high-resolution image of P4M1P taken at 4.2K and $M=60,000$. The OD pattern (the inset of the figure) shows reflections up to 220 (0.69nm spacing at room temperature). Clear (200) and (020) lattice fringes (0.97nm spacing at room temperature) are seen in the whole image, which intersect one another at an angle of 90° . No defects are recognized in this image. Another micrograph gives the reflection up to 420 (0.43nm spacing at room temperature) in its OD pattern.

PBPP single crystal

Figure 5 shows lath-shaped α -form single crystals of PBPP. The inset is the corresponding ED pattern of a multi-layered single crystal, which pattern was indexed based on the unit cell dimensions reported by Suzuki *et al.*²³: triclinic, $a'=1.66\text{nm}$, $b'=1.38\text{nm}$, $c(\text{chain axis})=0.98\text{nm}$, $\gamma'=97^\circ$ (here, the prime (') means the projected dimensions of the unit cell onto the plane normal to the chain axis). This $hk0$ net-pattern means that electron beams are incident upon the crystal in the direction parallel to the chain axis. The directional relationship between an image and its corresponding ED pattern hints that the long side-surfaces of the crystal are the $(1\bar{1}0)$ plane.

Figure 6 is a high-resolution image of a portion of the crystal in which two

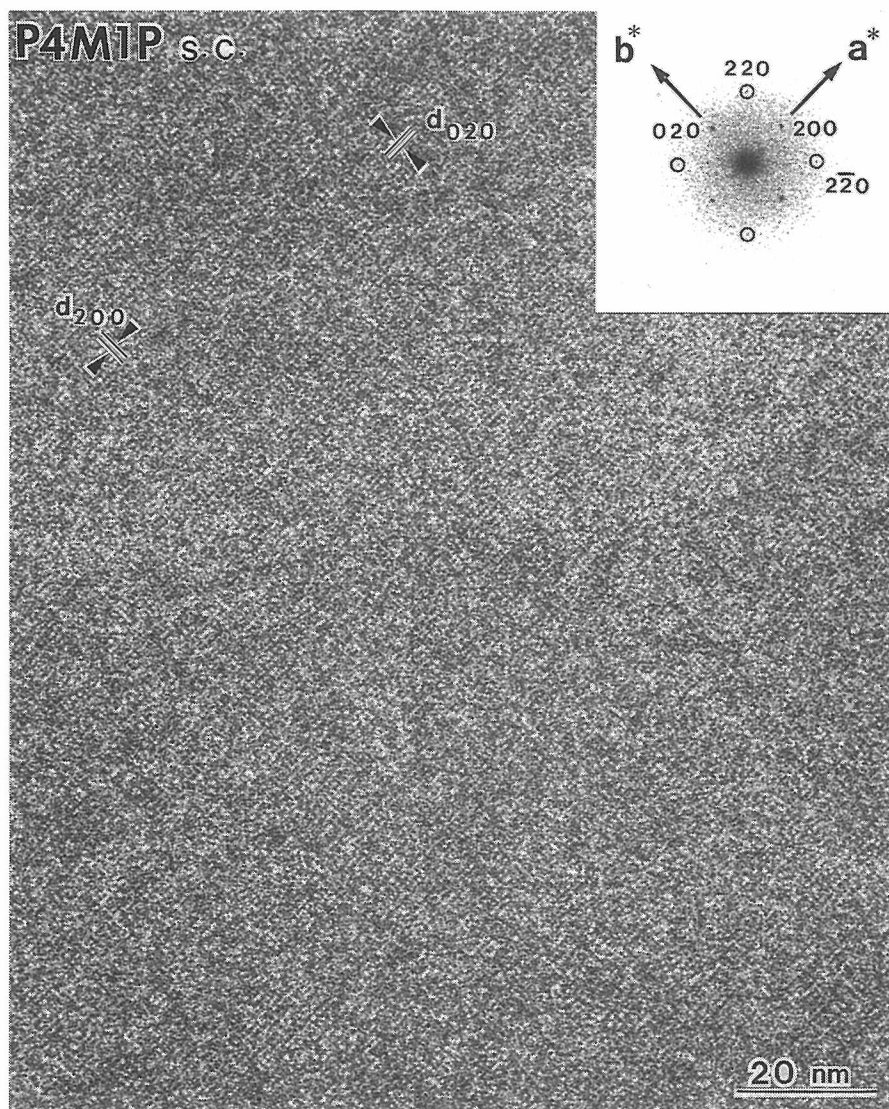


Fig. 4 High-resolution image of P4M1P form-III single crystal, which was taken at 4.2K and $M=60,000$. (200) and (020) lattice fringes are clearly seen in the image. The inset is the OD pattern of the image, showing the reflection up to 220 (0.69nm spacing at room temperature).

crystalline platelets of PBPP were coherently piled up. The image was taken at 4.2K and $M=60,000$. The thick arrow shows the edge of the superposed platelet. As judged from the direction of (110) lattice fringes (0.995nm spacing at room temperature) and also the corresponding OD pattern (the inset of the figure), it is concluded that the edge corresponds to the $(1\bar{1}0)$ plane although the edge winds in and out. The direction of long dimension of the lath-shaped crystal is, therefore, parallel to the $(1\bar{1}0)$ plane.

Figure 7 is another high-resolution image of PBPP, which was taken at 4.2K and

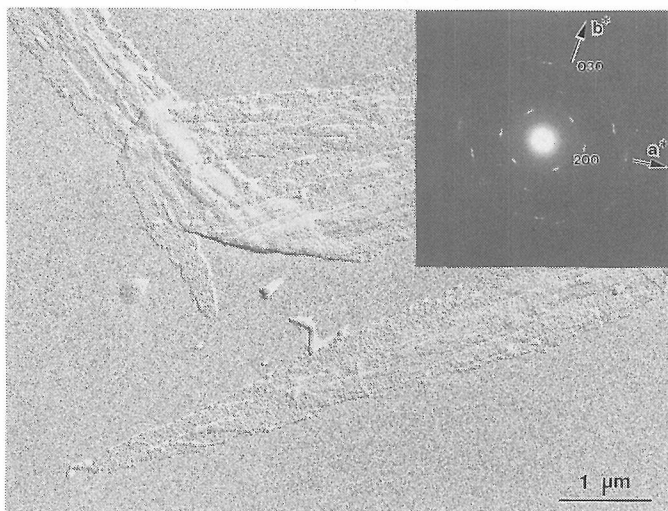


Fig. 5 PBPP α -form single crystal shadowed with Au. The inset is the ED pattern from a multi-layered lath-shaped crystal as shown in the lower half of the figure.

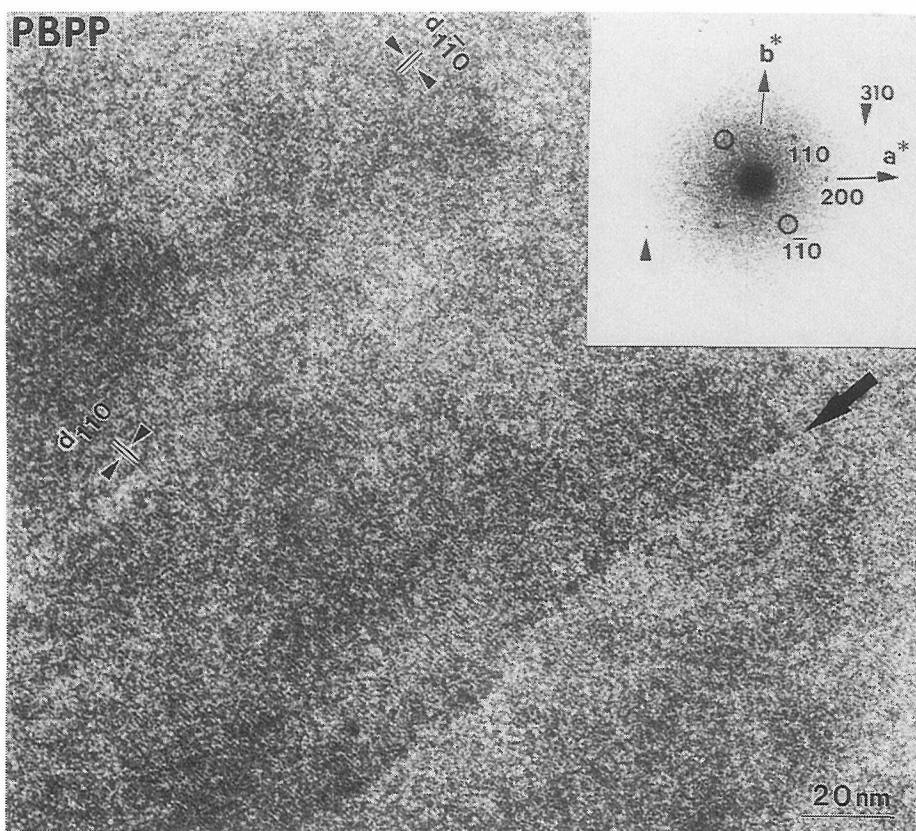


Fig. 6 High-resolution image of PBPP α -form single crystal, which was recorded at 4.2K and $M=60,000$. The thick arrow shows the edge of the superposed platelet. This image was taken at an appreciable amount of underfocus, so that the edge is easily recognized. The inset is the OD pattern of the image, showing reflections up to 310 (0.49nm spacing at room temperature).

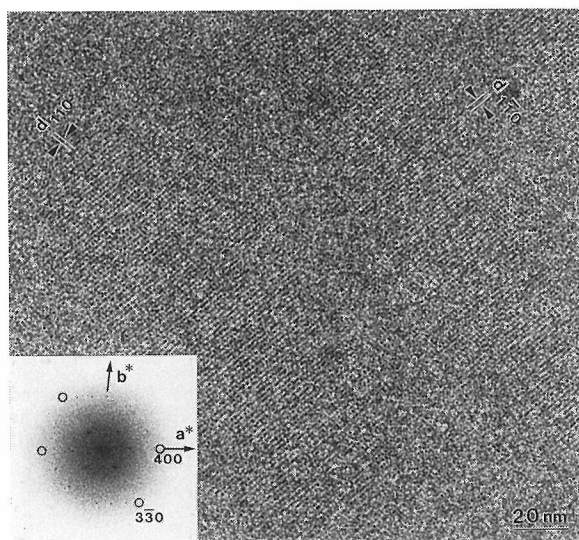


Fig. 7
High-resolution image of PBPP α -form single crystal, which was taken at 4.2K and $M=45,000$. The inset is the OD pattern of the image, showing the well-defined $hk0$ net-pattern with spot-like reflections up to $3\bar{3}0$ (0.37nm spacing at room temperature).

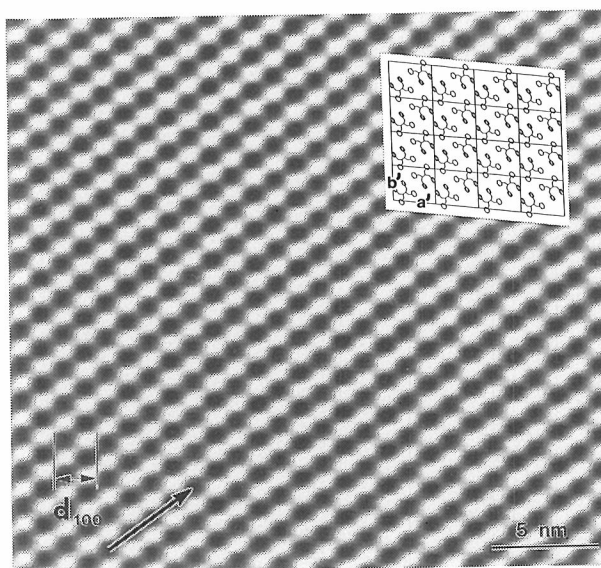


Fig. 8
Array of molecular images of PBPP α -form, which were obtained from Fig. 7 by computer Fourier filtering²⁴. Each dark dot corresponds to the PBPP molecular stem viewed along its axis. The inset is a model structure²³: $a'=1.66\text{nm}$, $b'=1.38\text{nm}$, and the angle γ' between a' and b' axes is 97° . The arrow indicates the direction parallel to the $(1\bar{1}0)$ lattice plane.

$M=45,000$. The inset is the corresponding OD pattern from the original negative, showing reflections up to $3\bar{3}0$ (0.37nm spacing at room temperature). In the image, distinct $(1\bar{1}0)$ fringes (1.123nm spacing at room temperature) and weak (110) fringes are observed, but others are not recognized due to a rather low signal-to-noise ratio [S/N]. To improve S/N, computer Fourier filtering²⁴ of the image in Fig. 7 was executed. Figure 8 is the resulted image indicating the array of molecules. The crystal structure of α -form PBPP has never been fully analyzed. The inset of Fig. 8 is a model proposed by Suzuki *et al.*, showing the crystal viewed in the direction parallel to the chain axis (c -axis)²³. Each dark dot in Fig. 8, thus, is attributed to the molecular stem viewed along its axis. Careful inspection of the image by viewing in the direction parallel to

(110) fringes, i.e., along the arrow in Fig. 8, reveals that the centers of individual dark dots align seemingly on a straight line but in a slightly zigzag fashion. This seems to indicate that the back-bone main chains are arranged in a similar zigzag fashion. Superposition of the model structure onto the image well demonstrates that the position of dark dots in the image is in good agreement with that of molecular stems in the model. At present, however, any images detailing directly the molecular shape of PBPP stems are not yet obtained.

CONCLUDING REMARKS

As mentioned in INTRODUCTION, there are two ways to increase the TEPD; (1) higher accelerating voltage of TEM, and (2) cryo-protection. The former way is not so advantageous for radiation-sensitive specimens, because both the image contrast and the sensitivity (speed) of photo-emulsion for image recording decrease with increasing voltage^{25,26}).

Cryo-protection for high-resolution TEM observation of polymer crystals was proved to be definitely effective at 4.2K using a cryo-TEM with a superconducting objective lens. The ratio $N_{4.2}/N_{RT}$ of more than 10 was confirmed¹⁸). High-resolution images of single crystals of PE, P4M1P and PBPP were successfully obtained at 4.2K using the cryo-TEM operated at 160kV. It is noticed, however, that the images reflect the structures at 4.2K, not those at room temperature. For example, the PE crystal lattice is different at low temperatures from that at room temperature: the dimensions a and b will decrease and c will slightly increase at low temperatures²⁷). The degree of contraction for both a and b of the single crystal measured with the cryo-TEM, nevertheless, was smaller than that estimated by an X-ray diffraction method: the a and b dimensions of PE single crystals used in this study were estimated as $a = 0.742\text{nm}$, $b = 0.496\text{nm}$ at room temperature, and $a = 0.735\text{nm}$, $b = 0.494\text{nm}$ at 4.2K. This is probably due to the effect of the support film for TEM experiments. The details will be reported elsewhere.

ACKNOWLEDGMENT

We thank Dr. R. St. John Manley (Pulp and Paper Research Institute of Canada and Department of Chemistry, McGill University, Montreal, Quebec, Canada) for the supply of P4M1P form-III single crystals, and Dr. M. Kojima (Chisso Corporation, Chiyoda-ku, Tokyo, Japan) for the supply of PBPP α -form single crystals.

REFERENCES

- (1) S. Isoda, M. Tsuji, M. Ohara, A. Kawaguchi and K. Katayama, *Polymer*, **24**, 1155(1983).
- (2) K. Katayama, S. Isoda, M. Tsuji, M. Ohara and A. Kawaguchi, *Bull. Inst. Chem. Res., Kyoto Univ.*, **62**, 198(1984).
- (3) H. Van der Werff, A.J. Pennings, G.T. Oostergetel and E.F.J. Van Bruggen, *J. Mater. Sci. Lett.*, **8**, 1231(1989).

- (4) H. Kawamura, M. Tsuji, A. Kawaguchi and K. Katayama, *Bull. Inst. Chem. Res., Kyoto Univ.*, **68**, 41(1990).
- (5) M. Tsuji, A. Uemura, M. Ohara, A. Kawaguchi, K. Katayama and J. Petermann, *Sen-i Gakkaishi*, **42**, T-580(1986).
- (6) J. Sugiyama, H. Harada, Y. Fujiyoshi and N. Uyeda, *Denshikenbikyo*, **20**, 143(1985).
- (7) J.-F. Revol, *Int. J. Biol. Macromol.*, **11**, 233(1989).
- (8) H.D. Chanzy, P. Smith and J.-F. Revol, *J. Polym. Sci.: Polym. Lett.*, **24**, 557(1986); S. Yamaguchi, M. Tatemoto and M. Tsuji, *Kobunshi Ronbunshu*, **47**, 105(1990).
- (9) H.D. Chanzy, P. Smith, J.-F. Revol and R.St.J. Manley, *Polym. Commun.*, **28**, 133(1987).
- (10) J.-F. Revol, K.H. Gardner and H. Chanzy, *Biopolymers*, **27**, 345(1988).
- (11) M. Tsuji, M. Ohara, S. Isoda, A. Kawaguchi and K. Katayama, *Phil. Mag. B.*, **59**, 393(1989).
- (12) J.-F. Revol, H.D. Chanzy, Y. Deslandes and R. H. Marchessault, *Polymer*, **30**, 1973(1989).
- (13) Y. Fujiyoshi, T. Kobayashi, K. Ishizuka, N. Uyeda, Y. Ishida and Y. Harada, *Ultramicrosc.*, **5**, 459(1980).
- (14) Handbook of "Low Dose Unit for EM400", Philips (1979).
- (15) G. Charlet, G. Delmas, J.F. Revol and R.St.J. Manley, *Polymer*, **25**, 1613(1984); G. Charlet and G. Delmas, *ibid.*, **25**, 1619(1984).
- (16) M. Kojima and J.H. Magill, *Polym. Commun.*, **24**, 329(1983).
- (17) M. Iwatsuki, H. Kihara, K. Nakanishi and Y. Harada, Proc. 11-th Int. Cong, EM, Kyoto, vol. 1, p. 251(1986).
- (18) M. Tsuji, M. Tosaka, A. Uemura, A. Kawaguchi, K. Katayama, M. Iwatsuki and Y. Harada, *Polym. Prepr., Japan*, **36**, 2357(1987); M. Tsuji, A. Uemura, M. Ohara, S. Isoda, A. Kawaguchi and K. Katayama, *Koenshu-Kyoto Daigaku Nippon Kagaku Sen'i Kenkyusho*, **44**, 1(1987).
- (19) E. Knapek, *Ultramicrosc.*, **10**, 71(1982).
- (20) H. Yamagishi, Y. Fujiyoshi, Y. Aoki, K. Morikawa, N. Uyeda and Y. Harada, *Denshikenbikyo*, **19**, 32(1984).
- (21) J.-F. Revol and R.St.J. Manley, *J. Mater. Sci. Lett.*, **5**, 249(1986).
- (22) P. Pradere, J.F. Revol, L. Nguyen and R.St.J. Manley, *Ultramicrosc.*, **25**, 69(1988).
- (23) A. Suzuki, H. Haruno, A. Takahashi and Y. Chatani, *Polym. Prepr., Japan*, **36**, 2351(1987).
- (24) M. Tsuji, S. Isoda, M. Ohara, K. Katayama and K. Kobayashi, *Bull. Inst. Chem. Res., Kyoto Univ.*, **55**, 237(1977).
- (25) K. Katayama, *Denshikenbikyo*, **21**, 181(1987).
- (26) M. Tsuji and K. Katayama, *Sen-i Gakkaishi*, **46**, P-388(1990).
- (27) A. Kawaguchi, R. Matsui and K. Kobayashi, *Bull. Inst. Chem. Res., Kyoto Univ.*, **55**, 217(1977).